Energy-Norm Based and Goal-Oriented Automatic hp Adaptivity for Electromagnetics. Application to Waveguide Discontinuities

Luis E. Garcia-Castillo, *Member, IEEE,* David Pardo and Leszek F. Demkowicz

***Abstract*—The Finite Element Method (FEM) enables the use of "adapted" meshes. The simultaneous combination of h (local variations in element size) and p (local variations in the polynomial order of approximation) refinements, i.e., hp-adaptivity, is the most powerful and flexible type of adaptivity. In this paper, two versions of a fully automatic hp-adaptive finite element method for electromagnetics are presented. The first version is based on minimizing the energy-norm of the error. The second, namely the goal oriented strategy, is based on minimizing the error of a given (user-prescribed) quantity of interest. The adaptive strategy delivers exponential convergence rates for the error, even in the presence of singularities. The hp adaptivity is presented in the context of two dimensional (2D) analysis of H-plane rectangular waveguide discontinuities. Stabilized variational formulations and $H(curl)$ FEM discretizations in terms of quadrilaterals of variable order of approximation supporting anisotropy and *hanging nodes* are used. Comparison of energy-norm and goal-oriented hp-adaptive strategies in the context of waveguiding problems is provided. Specifically, the scattering parameters of the discontinuity are used as goal.**

***Index Terms*—Finite element methods, waveguide discontinuities, rectangular waveguides**

I. Introduction

The Finite Element Method (FEM) is a powerful, accurate and flexible tool for the numerical solution of electromagnetic problems. In contrast to methods based on integral formulations, it can easily handle complex configurations of material constants (inhomogeneous media, anisotropy, etc.). It also enables the use of "adapted" meshes, not only to the geometry of the problem domain, but to the solution of the problem itself. Thus, very accurate solutions can be obtained, or equivalently, solutions with a given degree of accuracy using a minimum number of unknowns.

Specifically, when the adaption of the mesh to the solution is made automatically, it is referred to as automatic adaptivity or self-adaptive mesh refinements. That involves an iterative procedure in which a sequence of meshes is generated (typically by refining the previous mesh) using information about the error on the previous mesh. Self-adaptive procedures have additional advantages. They do not require any *a priori* knowledge of the solution of the problem under analysis, providing solutions with a user pre-specified degree of accuracy. Also, they simplify the costly (in terms of engineer time) task of generation of the mesh, since the mesh is automatically generated from an initial simple and coarse mesh.

There exist several types of adaptive procedures. The most common type is the h-adaptivity, in which the size of the finite elements (abstractly referred to as h) is modified in such a way that smaller elements are placed in the regions where the error is larger (an illustration is shown in Fig. 1). Without adaptivity, FEM provides rate of convergence for the solution equal to $O(h^{\min(p,k)})$ in terms of the energy norm, where p denotes the polynomial order of approximation within the finite elements, and k is a parameter that depends upon the smoothness of the solution. That is, the error is limited by the regularity of the solution. With h-adaptivity, the energy error of the solution is of N_{el}^{-dp} where N_{el} is the number of elements and $d = 2, 3$ is the dimension of the problem. Hence, h-adaptivity recovers the rate of convergence of the FEM for smooth solutions (case when $k > p$). The h-adaptivity is relatively common in the electrical engineering literature (e.g., references shown in [1]). A different type of adaptivity consists of varying the polynomial order of approximation p within a finite element, in such a way that higher p is chosen for the elements containing higher errors; thus, being referred to as p-adaptivity (an illustration is shown in Fig. 1).

For problems with singularities, the rate of convergence of the p-method (in terms of the total number of degrees-of-freedom (d.o.f.)) is twice the rate of h-adaptive methods. For problems with solutions that are analytical up to the boundary, the convergence is exponential. However, the above statement about p-adaptivity is only true for very smooth solutions, as the error is limited by the regularity of the solution k. Thus, if singularities are present (as in metallic or dielectric corners in the structure, certain interfaces between different media, etc.) the p-adaptivity does not present any advantage by itself. The p-adaptivity is much more uncommon than the h-adaptivity. One reason is probably the fact that p-adaptivity for electromagnetics requires the development of higher order curl-conforming (even div-conforming in some cases) finite element basis functions. In order to be practical for using different finite elements with different p in the mesh, basis functions need to be of hierarchical type. Such development has been (still is) an open issue in electromagnetics. In this context, an intensive research has been performed during the last two decades. Different higher order basis functions, mainly

L. E. Garcia-Castillo works at the Dep. Teoría de la Señal y Com., Univ. Carlos III de Madrid. Escuela Politécnica Superior (Edificio Torres Quevedo) Avda. de la Universidad, 30, 28911 Leganés (Madrid), Spain. luise@tsc.uc3m.es.

D. Pardo works at the Department of Petroleum and Geosystems Engineering, University of Texas at Austin, USA

L. F. Demkowicz works at the Institute for Computational Engineering and Sciences (ICES), University of Texas at Austin, USA

of interpolatory type, were first developed; see [1] and the references therein (up to 1998). Then, in the last decade, different implementations of higher order hierarchical finite elements were proposed. That opened the possibility of p-adaptivity. Thus, basis functions (up to third order) of [2] were used in [3]. A general framework for arbitrary order functions was presented in [4] with separation of gradients and rotational-like functions and special care in orthogonality properties. A similar approach, but modifying rotational functions to satisfy Nédélec conditions, is that of [5]. They were used in the implementation of p-refinements in [6], and [7], respectively. A family of hierarchical vector functions is also presented in [8] for multilevel algorithms [9]. A study of convergence under (uniform) p-refinements using basis of [10] (see also [11]) restriced to 2D is presented in [12].

The combination of h and p refinements, i.e., hp-adaptivity (an illustration is shown in Fig. 1), is the most powerful and flexible type of adaptivity. It provides exponential rates of convergence, even in the presence of singularities, in contrast to h and p schemes, in which algebraic rates of convergence are, in general, obtained. Thus, very accurate solutions can be obtained with an hp-adaptive strategy, even in the presence of singularities. Equivalently, approximate solutions within engineering accuracy can be obtained using a minimum number of unknowns. This is achieved by using large high order p elements in the regions where the solution is smooth and h-refinements with lower p towards the singularities. While some singularities can be determined a priori and special basis functions can be introduced to properly approximate them, [13], [14], [15], self-adaptive strategies, and specifically, of hp-type, are completely automatic and singularity independent. This is specially important for general electromagnetic problems. It is remarkable that, even for smooth solutions, the p-adaptivity alone is not enough. This is because the small features of the geometry require the use of small elements, i.e., h-adaptivity, to adapt the mesh to the geometry of the problem. Thus, independently of the theoretical considerations about the handling of singularities, the efficient analysis of practical microwave devices requires, in any case, the use of both, h and p, refinements.

By hp adaptivity we refer to adaptive schemes where h and p refinements are performed simultaneously in one step of the iterative process. Thus, we refer to rigorous hp schemes, in contrast to other approaches where in one step of the adaptivity only h or p refinements (but not both) are performed. The latter approaches might be better referred to as $h + p$ methods.

Adaptivity in hp is a technology that has been applied almost exclusively within the applied mathematics and computational mechanics communities [16]–[25]. The complexity of its implementation and mathematical analysis have precluded a wider use. With respect to hp-adaptivity for electromagnetic problems, extra technicalities come into play due to the particular characteristics of Maxwell's equations, in contrast to those of mechanics where the hp-adaptivity was first applied.

As mentioned above, self-adaptive procedures have important advantages. In this context, the authors have developed a fully automatic hp-adaptivity for electromagnetic problems, see [26] and the author references therein. A few other hp implementations for electromagnetics have been reported e.g., [27]–[29]. However, they lack many of the features of the implementation of the authors mentioned previously.

In this paper, we present a fully automatic hp-strategy applied to the two dimensional (2D) problem consisting on the analysis of H-plane rectangular waveguide discontinuities. The scope of the paper has been deliberately restricted to the H-plane case. Application of automatic hp-adaptivity to E-plane discontinuities can be found in a preliminary paper, [30]. The adaptive strategy is based on the projection of the interpolation error obtained from the solution on a "fine" grid. The strategy supports anisotropic refinements on irregular meshes with *hanging nodes*, and isoparametric as well as exact-geometry elements for one, two and three dimensional problems.

The adaptivity is usually formulated in such a way that the quantity to be optimized is the energy-norm of the error. The energy-norm is obtained from the variational formulation of the problem and, thus, it takes into account the error in the entire structure under analysis. The meshes provided by the adaptivity using this energy-norm approach are *equilibrated meshes*, i.e., meshes in which the error is balanced along the structure. This is useful to the microwave engineer as it assures a given pre-defined high-accuracy of the solution in the entire structure. Therefore, it is useful at aiming at finding optimum location and size of tuning elements (e.g., screws, dielectric posts, etc.). However, a microwave engineer is, typically, interested in the characterization of the structure in terms of its *scattering parameters* (*S-parameters*) which involves the solution of the problems only at the defined *ports* of the structure. Thus, an adaptivity driven by the minimization of given quantities, the S-parameters in this case, is desirable. This type of approach is called weighted residual method or goal-oriented method, [31]. Previous works on goal-oriented apporaches for S-parameters computation, e.g., [32], [33], have been mainly restricted to h-adaptivity.

In a previous work [30] results based on energy-norm adaptivity, but not with goal-oriented adaptivity, were presented. In this paper, both types of adaptivity, energy-norm based and goal-oriented, are presented. Comparison of energy-norm versus goal-oriented hp-adaptive strategies in the context of waveguiding problems is provided, showing their suitability for microwave engineering. To the authors best knowledge, this is the first paper containing an application of fully automatic hp-adaptivity to the analysis of microwave components and devices using both goal-oriented and energy-norm based approaches.

In this paper the 2D version of the hp-adaptivity is developed and used in the context of waveguiding problems. The reader interested on open region problems may refer to [34] that deals with Radar Cross Section modeling and radiation problems. A three dimensional (3D) version of the automatic hp-adaptivity can be found in [35]. However, complexity of 3D implementation of hp-adaptivity is much higher than that of 2D; not being yet at the same level of usability than the 2D implementation. The 3D implementation is under intensive development. The reader is referred to [36] for the most current work in 3D hp-adaptivity. In contrast to the present work,

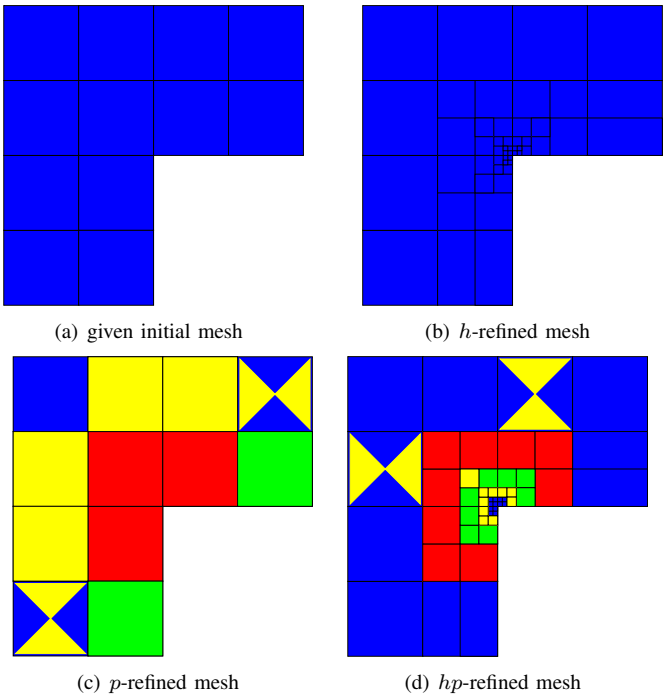

(a) given initial mesh (b) h-refined mesh

(c) p-refined mesh (d) hp-refined mesh

Figure 1. Different types of refinements. Color indicate the polynomial order p of the elements (blue being $p = 1$ and orange $p = 6$). Note: The meshes are simply for illustration purposes and they have not been obtained with any numerical code

3D deals exclusively with energy-norm adaptivity. Despite the final goal in the long run is 3D adaptivity, results of this paper are relevant for 3D computations too. This is due to the possibility to extend the 2D code to 3D by simply adding a one dimensional (1D) uniform grid, a Fourier transform, a Fourier series or modal expansion, in the third direction (as it is implicitly done in this paper to analyze H and E plane rectangular structures). In all these cases, the dramatic 2D savings in the number of unknowns (presented in the paper) automatically become 3D savings.

The implementation of the 2D hp-adaptivity utilizes a stabilized variational formulation (Section II) and hp-quadrangular elements of variable order (Section III) satisfying the "de Rham-diagram" commuting property [37]. The self-adaptive hp-algorithm is described in Section IV; specifically, the energy-norm version is presented in subsection IV-A, and the goal-oriented version in subsection IV-B. The numerical results presented in Section V confirm the exponentially fast decay of the error (as a function of the number of unknowns), as predicted by the theory. Also, advantages and disadvantages of goal-oriented based adaptivity (with the S-parameters as goal) are analyzed in comparison with energy-norm based adaptivity.

II. Variational Formulation

The analysis of a H-plane discontinuity can be two dimensional (2D) with a problem domain Ω corresponding to the cross-section obtained by intersecting the structure with the H-plane. A general H-plane discontinuity is shown in Fig. 2 for illustration purposes.

From Maxwell's equations, and considering the H-plane setup of Fig. 2 with TE_{10} excitation, $\partial/\partial z = 0$, we arrive at the following variational formulation:
Find $\mathbf{H}_\Omega \in \mathbf{W}$, $p \in V$ such that

$$c(\mathbf{F}_\Omega, \mathbf{H}_\Omega) = l(\mathbf{F}_\Omega), \qquad \forall \mathbf{F}_\Omega \in \mathbf{W} \tag{1}$$

where the functional space $\mathbf{W}$ is given by

$$\mathbf{W} := \{\mathbf{A} \in \mathbf{H}(\mathrm{curl}; \Omega),\ \hat{\mathbf{n}} \times \mathbf{A} = 0 \text{ on } \Gamma_D\} \tag{2}$$

and the sesquilinear and antilinear forms (c and l, respectively) are defined in (3). The over-bar means the complex-conjugate. $\mathbf{H}(\mathrm{curl})$ denotes the space of square integrable vector functions with square integrable curl.

$$\begin{aligned} c(\mathbf{F}_\Omega, \mathbf{H}_\Omega) = & \int_\Omega (\boldsymbol{\nabla} \times \bar{\mathbf{F}}_\Omega) \cdot (\frac{1}{\varepsilon_r} \boldsymbol{\nabla} \times \mathbf{H}_\Omega)\, d\Omega \\ & - k_o^2 \int_\Omega \bar{\mathbf{F}}_\Omega \cdot \mu_r \mathbf{H}_\Omega\, d\Omega \\ & + j \frac{k^2}{\varepsilon_r \beta_{10}} \int_{\sum_{\Gamma_p^i}} (\hat{\mathbf{n}} \times \bar{\mathbf{F}}_\Omega) \cdot (\hat{\mathbf{n}} \times \mathbf{H}_\Omega)\, d\Gamma \\ l(\mathbf{F}_\Omega) = & \ 2j \frac{k^2}{\varepsilon_r \beta_{10}} \int_{\Gamma_p^{\mathrm{in}}} (\hat{\mathbf{n}} \times \bar{\mathbf{F}}_\Omega) \cdot (\hat{\mathbf{n}} \times \mathbf{H}^{\mathrm{in}})\, d\Gamma \end{aligned} \tag{3}$$

In the above expressions, ε_r, μ_r are the electric permittivity and magnetic permeability, respectively, normalized with respect to the corresponding quantities for vacuum medium. Symbol k_0 stands for the vacuum wavenumber and β_{10} is the propagation constant of the TE_{10} mode. The unknown $\mathbf{H}_\Omega$ is related only to the two components of the magnetic field contained in the problem domain Ω, i.e., those parallel to the H-plane of the discontinuity. Analogously, the differential operator $\boldsymbol{\nabla}$ is referring only to the coordinates x, y of the H-plane. Boundary conditions are of Perfect Electric Conductor (PEC) on the walls of the waveguide, i.e., of Neumann type on Γ_N. A first order Absorbing Boundary Condition (ABC) with the mode impedance of the TE_{10} is used at the ports. The vector magnitude $\mathbf{H}^{\mathrm{in}}$ stands for the incident magnetic field of the TE_{10} mode at the port. Thus, is assumed that only the TE_{10} mode is present (with a non-negligible amplitude) at the ports (monomode propagation). Hence, the FEM domain should be truncated at a certain distance from the discontinuity. Note that a multimode boundary condition could have also been used. The monomode option has been chosen in this analysis for the sake of simplicity. Perfect Magnetic Conductors, i.e., Dirichlet type boundary condition on Γ_D, may be used as symmetry walls (not shown in Fig. 2).

The above variational formulation is not uniformly stable with respect to (angular) frequency ω. As $\omega \to 0$, i.e., $k_0 \to 0$, the term $k_o^2 \int_\Omega \bar{\mathbf{F}}_\Omega \cdot \mu_r \mathbf{H}_\Omega\, d\Omega$ becomes negligible compared with the curl-product term $\int_\Omega (\nabla \times \bar{\mathbf{F}}_\Omega) \cdot (\frac{1}{\varepsilon_r} \nabla \times \mathbf{H}_\Omega)\, d\Omega$. Thus, the problem becomes ill-posed, since the term with the product of the curls does not "see" the gradients, and the gradients remain undetermined in the zero frequency limit. Moreover, this low frequency breakdown problem is not only related to the situation of $\omega \to 0$, but, in general, to the relative size of the finite elements compared with the wavelength λ. It can

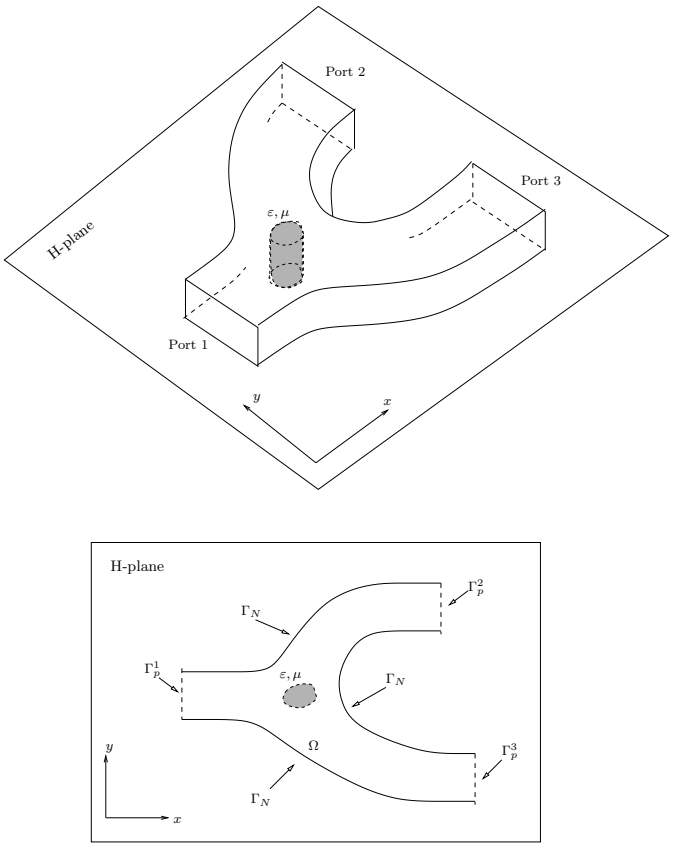

Figure 2. A rectangular H-plane discontinuity and its 2D FEM modeling. No Perfect Magnetic Conductor (Γ_D) boundary is used in this case.

be easily seen (by considering uniform h-refinements over a given mesh) that the ratio of the term $k_o^2 \int_\Omega \bar{\mathbf{F}}_\Omega \cdot \mu_r \mathbf{H}_\Omega \, d\Omega$ to the curl-product term $\int_\Omega (\nabla \times \bar{\mathbf{F}}_\Omega) \cdot (\frac{1}{\varepsilon_r} \nabla \times \mathbf{H}_\Omega) \, d\Omega$ is $(k_0 h)^2$, i.e., proportional to $(h/\lambda)^2$. Therefore, even far from the low frequency region, when very small elements are used (as it is the case for h or hp adaptivity) the low frequency breakdown situation may be present.

As a remedy to this problem, a Lagrange multiplier p is introduced to enforce the weak form of the continuity equation (obtained by employing gradients as test functions in (1)). Thus, the *stabilized* variational formulation with the Lagrange multiplier is given by:

Find $\mathbf{H}_\Omega \in \mathbf{W}$, $p \in V$ such that

$$\begin{aligned} c(\mathbf{F}_\Omega, \mathbf{H}_\Omega) + b(\mathbf{F}_\Omega, \nabla p) &= l(\mathbf{F}_\Omega) \qquad \forall \mathbf{F}_\Omega \in \mathbf{W} \\ b(\nabla q, \mathbf{H}_\Omega) &= g(\nabla q) \qquad \forall q \in V \end{aligned} \tag{4}$$

where the space V is defined as

$$V := \{p \in H^1(\Omega),\ p = 0 \text{ on } \Gamma_D\} \tag{5}$$

and the new sesquilinear and antilinear forms, b, and g, respectively, are defined in (6). H^1 denotes the space of square integrable functions with square integrable first derivative.

$$\begin{aligned} b(\mathbf{F}_\Omega, \boldsymbol{\nabla} p) = &- k_o^2 \int_\Omega \bar{\mathbf{F}}_\Omega \cdot \mu_r \boldsymbol{\nabla} p \, d\Omega \\ &+ j \frac{k^2}{\varepsilon_r \beta_{10}} \int_{\sum_i \Gamma_p^i} (\hat{\mathbf{n}} \times \bar{\mathbf{F}}_\Omega) \cdot (\hat{\mathbf{n}} \times \boldsymbol{\nabla} p) \, d\Gamma \\ g(\boldsymbol{\nabla} q) = &\, 2j \frac{k^2}{\varepsilon_r \beta_{10}} \int_{\Gamma_p^{\text{in}}} (\hat{\mathbf{n}} \times \boldsymbol{\nabla} \bar{q}) \cdot (\hat{\mathbf{n}} \times \mathbf{H}^{\text{in}}) \, d\Gamma \end{aligned} \tag{6}$$

By substituting $\mathbf{F}_\Omega = \boldsymbol{\nabla} q$, $q \in V$ in the above formulation (4), we infer that the Lagrange multiplier p satisfies the weak form of a Laplace-like equation. Thus, if (homogeneous) Dirichlet boundary conditions are present ($\Gamma_D \neq 0$), i.e., when symmetry walls are used in the analysis, the Lagrange multiplier p identically vanishes. Note that the multiplier p is undefined when $\Gamma_D = 0$ (it is a constant but undefined function over Ω). In that case, after the FEM discretization, one degree of freedom of p is set to a given value (typically zero). Thus, the multiplier p identically vanishes for $\Gamma_D = 0$. The stabilized formulation works because the gradients of scalar-valued potentials from V form precisely the null space of the curl on vector functions in $\mathbf{H}$. This condition shall be preserved at the discrete level by a careful construction of the finite element basis. Notice that $b(\mathbf{F}_\Omega, \nabla p)$ and $g(\nabla q)$ should both be divided by k_o.

The scattering parameters of the structure (monomode, TE_{10}) are obtained as

$$S_{ii} = \frac{\displaystyle\int_{\Gamma_{p_i}} \mathbf{H}_\Omega(\xi) \cdot \sin \frac{\pi \xi}{a^{p_i}} \, \mathbf{d\Gamma}_{p_i}}{H_0^{\text{in}} \dfrac{a^{p_i}}{2}} - 1 \tag{7}$$

and,

$$S_{ji} = \frac{\sqrt{Z_{\text{TE}_{10}}^{p_j}} \displaystyle\int_{\Gamma_{p_j}} \mathbf{H}_\Omega(\xi) \cdot \sin \frac{\pi \xi}{a^{p_j}} \, \mathbf{d\Gamma}_{p_j}}{H_0^{\text{in}} \dfrac{a^{p_i}}{2} \sqrt{Z_{\text{TE}_{10}}^{p_i}}} \tag{8}$$

where a^{p_i} refers to the broad dimension of the waveguide at port i, and H_0^{in} is the amplitude of $\mathbf{H}^{\text{in}}$. Symbol ξ refers to a coordinate axis local to the port and $Z_{\text{TE}_{10}}^{p_i}$ stands for the impedance of the mode. Note that S_{ii} of (7) corresponds to a definition with respect to admittance. A minus sign should be added to (7) for a S_{ii} definition with respect to impedance.

III. hp Discretization

To discretize the above variational formulations, we introduce finite dimensional spaces $\mathbf{W}_{hp} \subset \mathbf{W}$, and $V_{hp} \subset V$, where h denotes the element size, and p the polynomial order of approximation. These spaces have been constructed to verify the following condition at the discrete level: $\boldsymbol{\nabla} \times \mathbf{F} = 0, \mathbf{F} \in \mathbf{W}_{hp}$ if and only if $\exists\, q \in V_{hp} : \mathbf{F} = \boldsymbol{\nabla} q$. This condition is essential in order to satisfy the commutativity property of the so-called "de Rham" diagram [37]. This commutativity property, which is essential to guarantee a proper stability and convergence properties of the resulting method, implies that V_h is of order $p+1$, where p is the order of approximation of $\mathbf{W}_h$. Thus, from a set of basis functions associated to space $V_{h,p+1}$ we construct the corresponding basis for $\mathbf{W}_{hp}$.

A detailed construction of a proper set of basis functions can be found in [26] for triangles and quadrilaterals. In this paper, we have employed quadrilaterals because they are appropriate to model structures in rectangular waveguide technology.

We employ hierarchical basis functions, which facilitates the use of conforming approximations among finite elements of different order p. In addition, we support irregular meshes, i.e., meshes with *hanging nodes*, which appear naturally during h-refinements. A 2D mesh is irregular if the edge of a given (larger) element is shared by more than one (smaller) neighbour. Examples of irregular meshes are those of Figures 1(b) and 1(d). As a consequence, the nodes associated to the edges of the small neighbours are *constrained* by the common edge of the larger element. These nodes are the so-called *constrained nodes* or *hanging nodes* (see [26] for details). Basis functions are defined over a master element. A change of coordinates is used to express these functions over the physical element.

IV. Automatic hp Adaptivity

A. Energy-Norm based Adaptivity

Given an initial regular (without hanging nodes) hp-grid, the self-adaptive strategy automatically generates a sequence of optimal hp-grids providing exponential convergence rates in terms of the energy-norm error (or the given quantity of interest as shown next in subsection IV-B) vs. the number of unknowns (and CPU time). The refined grids are 1-irregular meshes, i.e., the parent of a h-refined element is not allowed to have *hanging nodes*. Thus, the algorithm enforces uniform refinements in the parent element to satisfy this condition. Thus, h-refinements are kept local (see examples of Figures 1(b) and 1(d), and the meshes shown in Section V).

The details of the self-adaptive strategy are quite involved and can be found in [26]. A "competition" between p-refinement with all *competitive* h-refinements takes place at each iteration step. Competitive h-refinements are those that result in the same increase in the number of d.o.f. as the p-refinement. Thus, the use of error indicators is not enough. The error function needs to be known (or estimated) in order to decide how to refine the mesh at each iteration step. In this context, a key ingredient is the projection based interpolation operator for H^1-spaces and $\mathbf{H}(\text{curl})$-spaces, [26]. This local operator preserves conformity in the sense of the working space, i.e., continuity of the (scalar) function for H^1-spaces and continuity of the tangential components for $\mathbf{H}(\text{curl})$-spaces. Furthermore, it has been proven that, given a solution on the continuous space, it produces an approximation of the solution in a discrete space that is asymptotically optimal with respect both h and p. Thus, given the exact solution, it allows for comparison of optimal h- and p-refinements without the need of solving thousands of global discrete problems. The exact solution is approximated by employing a fine grid solution. Thus, in order to find optimal refinements for a given hp-grid, we first solve the problem over the globally refined $h/2, p+1$ grid (fine grid), which is obtained from the hp-grid by a global h- and p-refinement. Hence, we use the $h/2, p+1$-grid solution as the reference solution to produce our next optimal $\hat{hp}$-grid, which is an intermediate grid between the hp and $h/2, p+1$-grids. The "competition" is driven by the *error decrease rate* of each edge of the mesh; being equal to

$$\frac{\|\mathbf{H}_{h/2,p+1} - \mathbf{\Pi}^{curl}_{hp}\mathbf{H}\| - \|\mathbf{H}_{h/2,p+1} - \mathbf{\Pi}^{curl}_{\hat{hp}}\mathbf{H}\|}{(p_1 + p_2 - p)}\,, \tag{9}$$

where $\mathbf{\Pi}^{curl}\mathbf{H}$ stands for the projection based interpolation of $\mathbf{H}$ and $\hat{hp} = (\hat{h}, \hat{p})$ is such that $\hat{h} \in \{h, h/2\}$. If $\hat{h} = h$, then $\hat{p} = p+1$. If $\hat{h} = h/2$, then $\hat{p} = (p_1, p_2)$, where $p_1+p_2-p > 0$, $\max\{p_1, p_2\} \leq p+1$.

The error (to be minimized) is measured with the energy-norm of the problem (denoted as $\|\cdot\|$) that is obtained from an "energy" type inner product defined over $\mathbf{W}$. For instance, the energy-norm of $\mathbf{H} \equiv \|\mathbf{H}\| = \sqrt{\langle \mathbf{H}, \mathbf{H} \rangle}$, where the inner product is given by:

$$\begin{aligned}\langle \mathbf{F},\mathbf{H} \rangle = &\int_\Omega (\boldsymbol{\nabla} \times \bar{\mathbf{F}}) \cdot (\frac{1}{\varepsilon_r} \boldsymbol{\nabla} \times \mathbf{H})\, d\Omega \\ &+ k_o^2 \int_\Omega \bar{\mathbf{F}} \cdot \mu_r \mathbf{H}\, d\Omega \\ &+ \left| j \frac{k^2}{\varepsilon_r \beta_{10}} \right| \int_{\sum_{\Gamma_p^i}} (\hat{\mathbf{n}} \times \bar{\mathbf{F}}) \cdot (\hat{\mathbf{n}} \times \mathbf{H})\, d\Gamma\end{aligned} \tag{10}$$

The contribution to the energy-norm of the Lagrange multiplier p (in the case of the stabilized formulation) is not considered as the multiplier p is identically null. The energy norm inferred by (10) takes into account the phsysics of the problem. However, the differences in the results when using the mathematical norm of the space of the solution, i.e., $H curl$ norm, have shown to be very small, at least for the particular structures analyzed in Section V.

Note that the subindex Ω has been omitted for the sake of clarity of the expressions (as will be done in the remainder of the paper).

B. Goal-Oriented Adaptivity

It will be assumed that there is a quantity of interest that can be expressed as a continuous and linear functional L. By recalling the linearity of L,

$$\text{Error of interest} = L(\mathbf{H}) - L(\mathbf{H}_{hp}) = L(\mathbf{H} - \mathbf{H}_{hp}) = L(\mathbf{e}) \tag{11}$$

where $\mathbf{H}_{hp} \in \mathbf{W}_{hp}$ and, $\mathbf{e}$ denotes the error function.

By defining the residual $\mathbf{r}_{hp}(\mathbf{F}) = l(\mathbf{F}) - c(\mathbf{F}, \mathbf{H}_{hp}) = c(\mathbf{F}, \mathbf{H} - \mathbf{H}_{hp}) = c(\mathbf{F}, \mathbf{e})$, we look for the solution of the *dual problem*:

$$\begin{cases} \text{Find } \bar{\mathbf{H}}^d \in \mathbf{W} \\ c(\mathbf{H}^d, \mathbf{F}) = L(\mathbf{F}) \quad \forall \mathbf{F} \in \mathbf{W} \end{cases} \tag{12}$$

Problem (12) has a unique solution in $\mathbf{W}$, $\mathbf{H}^d$, which is usually referred to as the *influence function*. The hp-discretized version of (12) is solved obtaining $\mathbf{H}^d_{hp} \in \mathbf{W}_{hp}$.

Definition of the dual problem plus the Galerkin orthogonality condition for the original problem imply the final

representation formula for the error in the quantity of interest, namely,

$$L(\mathbf{e}) = c(\mathbf{e}, \mathbf{H}^d) = c(\mathbf{e}, \underbrace{\mathbf{H}^d - \mathbf{H}^d_{hp}}_{\boldsymbol{\epsilon}}) = \tilde{c}(\mathbf{e}, \boldsymbol{\epsilon}) \tag{13}$$

where $\tilde{c}(\mathbf{e}, \boldsymbol{\epsilon}) = c(\mathbf{e}, \bar{\boldsymbol{\epsilon}})$ denotes the bilinear form corresponding to the original sesquilinear form.

Once the error in the quantity of interest has been determined in terms of bilinear form $\tilde{c}$, we wish to obtain a sharp upper bound for $|L(\mathbf{e})|$ that depends upon the mesh parameters (element size h and order of approximation p) only locally. Then, a self-adaptive algorithm (similar to the one with the energy-norm) may be constructed. As in the energy-norm based approach, a fine grid is used. The solutions, $\mathbf{H}$, $\mathbf{H}^d$, are approximated by the fine grid solutions, $\mathbf{H}_{\frac{h}{2},\, p+1}$, $\mathbf{H}^d_{\frac{h}{2},\, p+1}$. Thus, in the remainder of this article, $\mathbf{H}$ and $\mathbf{H}^d$ will be used to denote the fine grid solutions of the direct and dual problems.

Next, the error in the quantity of interest is bounded by a sum of element contributions. Let b_K denote a contribution from element K to sesquilinear form c. It then follows that

$$|L(\mathbf{e})| = |c(\mathbf{e}, \boldsymbol{\epsilon})| \leq \sum_K |c_K(\mathbf{e}, \boldsymbol{\epsilon})| \tag{14}$$

where summation over K indicates summation over elements.

Now, the projection based interpolation comes into play as it does in the energy-norm approach. Then, following an approach similar to the one of [38], an upper bound for $|L(\mathbf{e})|$ is obtained:

$$|L(\mathbf{e})| \leq C \sum_K \|\tilde{\mathbf{e}}\|_K \|\tilde{\boldsymbol{\epsilon}}\|_K \tag{15}$$

where C is a positive constant (typically, close to one), and $\|\cdot\|_K$ denotes the energy-norm restricted to element K. Symbols $\tilde{\mathbf{e}}$, $\tilde{\boldsymbol{\epsilon}}$ correspond to the projection based interpolation errors on $\mathbf{H}$ and $\mathbf{H}^d$, respectively.

Thus, the goal-oriented adaptivity is an extension of the energy-norm based adaptivity in which the refinements are guided by the errors, not only on the primal variable $\mathbf{H}$, but also on the *influence function* $\mathbf{H}^d$. Notice that, in practice, the computational cost of solving the dual problem is small. The linear system of equations is factorized only once, and the extra cost of solving the dual problem reduces to only one backward and one forward substitution (if a direct solver is used).

1) Goal-Oriented Adaptivity with S-Parameters: A quantity of interest must be decided first (in this case, a particular S-parameter). Typically, there are certain relations that are satisfied by the S-parameters when considering waveguide discontinuities. For instance, due to the reciprocity of the electromagnetic field, $S_{ji} = S_{ij}$. This equality is also satisfied at the discrete level, since the reciprocity is satisfied by the variational formulation of the problem. Thus, the use of the goal-oriented adaptivity with S_{ji} or S_{ij} as our quantity of interest will provide identical grids and results. Also, it is usual to have certain symmetries in the structure, reducing the number of independent S-parameters. For instance, it may happen that $S_{11} = S_{22}$. However, $S_{11} = S_{22}$ only holds at the discrete level if the initial grid is also symmetric. Thus, in this case, the use of the goal-oriented adaptivity with S_{11} or S_{22} as our quantity of interest, will provide identical grids and results provided that the initial grid is symmetric. Specifically, for lossless structures (which is a common idealization in many waveguiding problems) we know that the S-matrix is unitary, which implies a considerable number of relations between the S-parameters. Note, however, that at the discrete level the S-matrix is not longer unitary. Actually, the higher number of degrees of freedom (lower error of the solution) the better approximation of unitariness of the computed S-matrix.

In the case of a two port symmetric structure, we need to choose between S_{11} and S_{21} as our quantity of interest. Notice that $S_{11}(\mathbf{H})$ is not a linear functional. However, $L_1(\mathbf{H}) = S_{11}(\mathbf{H}) + 1$ is a linear and continuous functional, and therefore, we may use it as our quantity of interest for the goal-oriented optimization algorithm. It is important to note that $L_1(\mathbf{H})$ is equal (up to a multiplicative constant) to the functional l representing the right hand side of the original problem. Thus, solution of the dual problem $\mathbf{H}^d$ is also equal (up to a multiplicative constant) to the solution of the original problem $\mathbf{H}$. For this particular case, the goal-oriented adaptivity coincides exactly with the energy driven adaptivity, and the corresponding numerical results are identical (also observed by [33]). In other words, for the waveguide discontinuity problem, energy-norm adaptivity is optimal for computing S_{11}.

V. Numerical Results

Numerical results for three H-plane structures are given: one structure with a severe field singularity, one with a small feature, and other with a smooth field solution. The third serves to illustrate the features of goal-oriented adaptivity in comparison with the energy-norm based approach. Results for E-plane discontinuities with the energy-norm can be found in [30].

First, we describe numerical results showing the exponential type of convergence for the error (in the energy norm), even in the presence of field singularities. By exponential convergence it is meant that error $= C\exp(-N_{\text{dof}}^{\alpha})$ in the asymptotic regime, N_{dof} being the number of unknowns. Specifically, the theory according to [39] predicts that $\alpha = 1/3$ for 2D. Thus, the exponential convergence behavior is shown as a straight line when plotting the error in logarithmic scale versus $N_{\text{dof}}^{1/3}$. This is precisely how the scales of the plots shown in the paper have been set up. Note that the abscissa scale corresponds to $N_{\text{dof}}^{1/3}$ while abscissa axis tics should be read as N_{dof} in the plots.

A zero length septum (i.e., transverse to the wave propagation) is considered. The dimension of the septum is 0.1 and is centered with respect to the waveguide (of dimensions 1x0.5). Note that the length units are normalized. The initial mesh is shown in Fig. 3, in which the colors indicates, according to the scale on the right, the order p of the elements (the dark blue being $p = 1$ and the pink $p = 9$) It is important to note that the order corresponds to the H^1 Lagrange multiplier, and the field of $\mathbf{H}(\text{curl})$ is of order $p-1$. In this case, all elements are of order 3 for the Lagrange multiplier and order 2 for the magnetic field. The analysis is made by exciting the port on

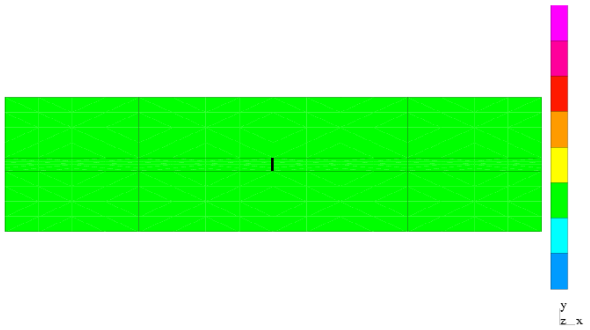

Figure 3. Initial mesh for the H-plane zero length septum. For illustration purposes, the septum is added to the plot with finite length

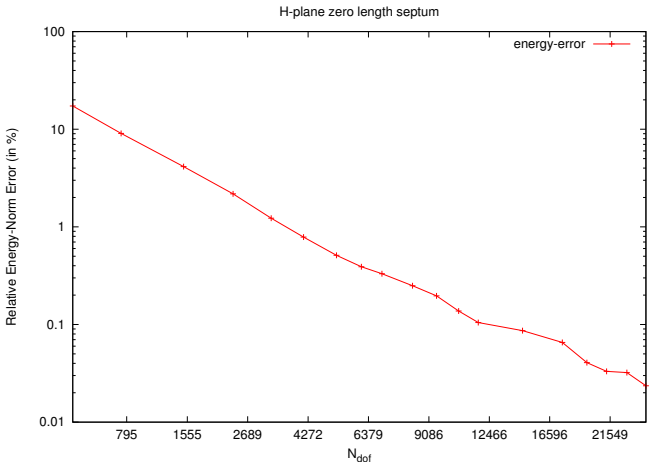

Figure 4. Convergence history for the H-plane zero length septum

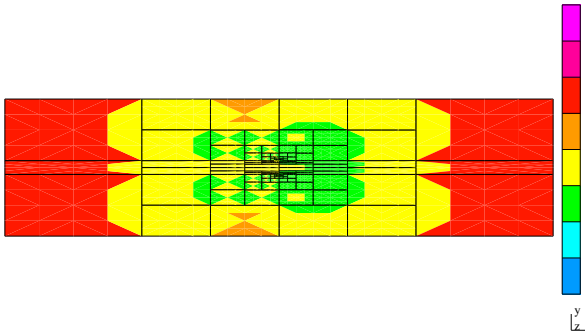

Figure 5. 7th mesh for the H-plane zero length septum

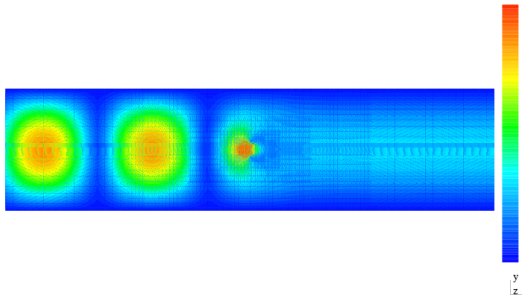

Figure 6. Magnitude of H_y corresponding to the H-plane zero length septum

the left with a TE_{10} wave of frequency equal to 1.5 times its cut-off frequency. The convergence history is shown in Fig. 4, where it is observed that, after a few iterations (due to a deliberate coarseness of the initial mesh), exponential convergence of the error is obtained. Figure 5 shows an example of hp-mesh provided by the automatic energy-norm adaptivity. As predicted by the theory, h-refinements are observed towards the corners where there is a singular behavior of the field, and p-refinements in the regions where the field variation is smooth.

A plot of $|H_y|$ is shown in Fig. 6, in which a stationary wave pattern at the input waveguide and singular behavior of the field at the septum corners is observed. The results for S_{11} and S_{21} corresponding to four non-consecutive iterations of the hp adaptivity are shown in Tab. I together with those obtained with Mode Matching. For iterations higher than the 11th, the error obtained with the hp-adaptivity is presumed to be lower than the one delivered by the Mode Matching technique; thus, results for higher iteration numbers are omitted. This is concluded after selecting a higher number of modes in the modal expansions and observing fluctuations at the fifth digit level of the values of the S-parameters.

A H-plane T-junction with metallic post, specifically the one of [40, Fig. 2], is considered next. The initial mesh is shown in Fig. 7. The convergence history is shown in Fig. 8. Exponential convergence of the error is observed. Figure 9 shows an example of hp-mesh provided by the automatic adaptivity. Refinements on p are observed in the waveguide sections. Note than, although there is no field singularity, the strong variation of the fields around the post and the small feature that it represents inside the junction, force h refinements around the post. Results shown above correspond to the excitation of the port on the top (port 1) with a TE_{10} wave of frequency equal to 11.5 GHz (1.75 times its cut-off frequency). The reflection coefficient S_{11} frequency response is shown in Fig. 10 for two different error thresholds of the automatic adaptivity.

The next example is a H-plane structure consisting of a multisection impedance-matched dielectric-slab filled-waveguide phase-shifter, published in [41] (the dimensions on the H-plane are shown in Fig. 11; the waveguide is 7.112x3.556). The field solution of the structure is smooth, since there is no field singularity in this case. Thus, hp-adaptive strategy is expected to deliver an increase in the polynomial order of approximation p. Note that that h refinements appear due to the limitation on the maximum p of the implementation ($p = 9$). Thus, the order p is increased until the maximum p is reached in the fine grid; from this moment, h-refinements are selected until the specified error criterion is satisfied. Therefore, the exponential convergence is not achieved in this case (it would require very high p). However, hp-adaptivity shows a much higher rate of convergence than h-adaptivity, as illustrated in Fig. 12, where rates of convergences for h-adaptivity with fixed $p = 1$ and fixed $p = 2$ are shown. The abscissa axis

Table I
SCATTERING PARAMETERS FOR THE H-PLANE ZERO LENGTH SEPTUM (MM STANDS FOR MODE MATCHING)

	$\|S_{11}\|$	$\|S_{21}\|$	$\arg(S_{11})$	$\arg(S_{21})$
Iter. 2	0.7200	0.6939	50.520°	-37.987°
Iter. 5	0.7817	0.6236	56.432°	-33.550°
Iter. 8	0.7883	0.6153	57.042°	-32.962°
Iter. 11	0.7896	0.6136	57.165°	-32.840°
MM	0.7897	0.6135	57.171°	-32.829°

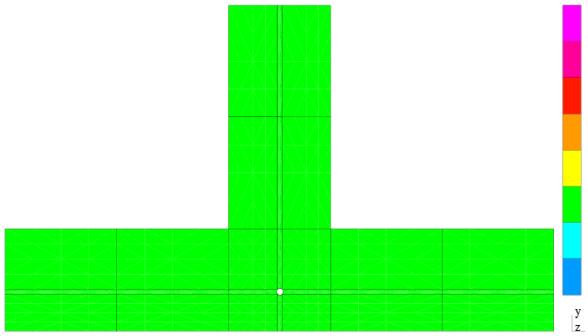

Figure 7. Initial mesh for the H-plane T-junction with metallic post. WR90 waveguides (22.86mm x 10.16mm). Post shifted 0.1mm right and 2.63mm down with respect to junction center

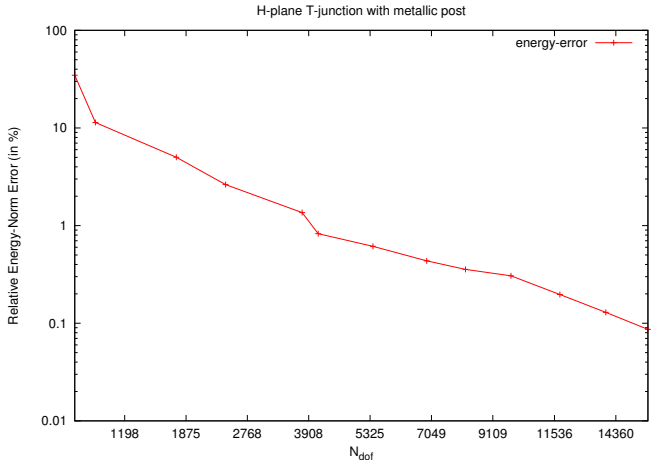

Figure 8. Convergence history for the H-plane T-junction with metallic post

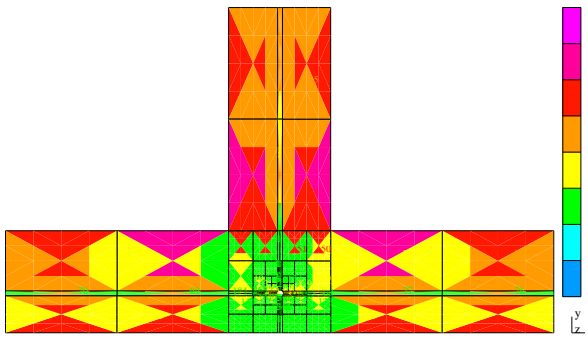

Figure 9. 5th mesh for the H-plane T-junction with metallic post

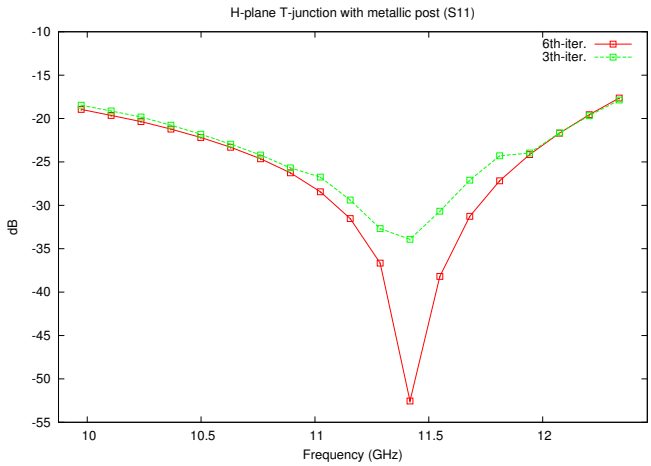

Figure 10. Frequency response of H-plane T-junction with metallic post ($|S_{11}|$ in dB). 3th and 6th- iterations correspond to error around 5% and 1%, respectively

is in log-type scale. Notice that hp-adaptivity requires only 7,000 unknowns to accurately solve the problem, in contrast with around 150,000 unknowns needed by h-adaptivity with $p = 2$. The h-adaptivity with $p = 1$ is simply not able to reach, in practice, a reasonable accuracy (with 100,000 unknowns the error is still over 25%). Thus, a dramatic saving is achieved by using hp-adaptivity. These savings are even larger when compared with the case of no adaptivity. As it was mentioned in the Introduction, this savings in unknowns for 2D domains automatically become savings for some 3D structures suitable to be analyzed by simply adding a 1D uniform grid, a 1D Fourier transform, a 1D Fourier series, or a 1D modal expansion in the third direction.

This structure serves to illustrate the features of the goal-oriented adaptivity. The convergence comparison between energy-norm based adaptivity and goal-oriented with S_{21} as the quantity of interest is shown in Fig 13. Note that goal-oriented adaptivity with S_{11} provides identical results to the energy-norm based adaptivity, as explained in sub-section IV-B1. It is observed how both types of adaptive strategies provide very similar results. This is due to the strong relation between S_{21} and S_{11} for this case (lossless case). However, in other cases where S_{21} is not so strongly related to S_{11}, the goal-oriented with S_{21} is expected to provide much better results than energy-norm based approach. Possible scenarios of this situation are structures with many ports, or the presence of significant losses within the structure. As an example of the latter, losses in the dielectric-slab of the structure have been added (serving as an illustration of an attenuator type of structure). Several values of the loss tangent of the dielectric ($\tan\delta$) material of the waveguide have been considered. As the dielectric losses are higher, the differences between goal-oriented adaptivity and energy-norm based adaptivity increase. Results for $\tan\delta = 1$ are shown in Fig. 14, in which we observe that the 1% error level requires less than 3000 unknowns with goal-oriented, while the energy-norm with 24000 unknowns still provides an error larger than 3%.

It is very instructive to see the hp-grids delivered by both

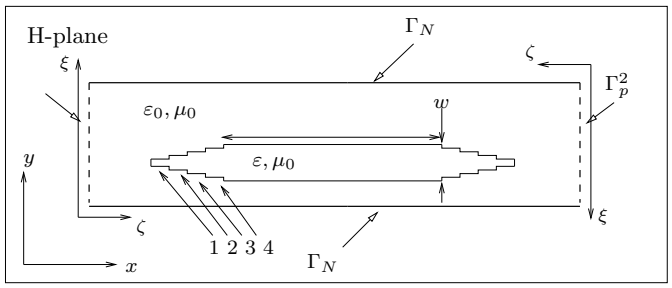

Figure 11. Dielectric-slab filled waveguide structure (Data from [41]: l=24.50, w=2, l_1=3.414, w_1=0.194, l_2=3.163, w_2=0.646, l_3=2.852, w_3=1.2, l_4=2.6, w_4=1.742)

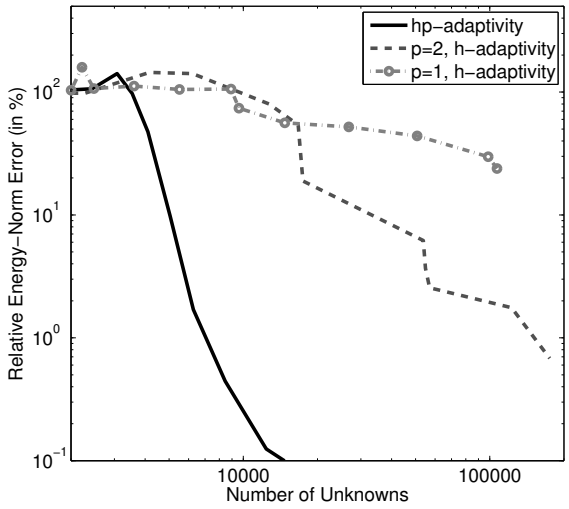

Figure 12. Convergence histories for hp and h adaptive strategies for the dielectric-slab filled waveguide

types of adaptivity for the lossy case with $\tan\delta = 1$. Figure 15 shows the hp-grids for energy-norm based and goal-oriented adaptive strategies. Energy norm adaptivity concentrates the unknowns near the incident port (on the left) as most of the energy is in that region. However, the goal-oriented adaptivity is driven also by the error of the dual problem, i.e., by considering $L_2(\mathbf{H}) = S_{21}$ as the excitation. From (8), we observe that the excitation of the dual problem is at the transmitted port (at the right). Thus, the goal-oriented grid shows a symmetric pattern.

VI. Conclusions

Energy-norm based and goal-oriented hp-adaptive strategies have been presented in the context of the 2D analysis of H-plane rectangular waveguiding discontinuities. Exponential rates of convergence, even in the presence of singularities, have been achieved. Thus, very accurate solutions are obtained with a minimum number of unknowns. The hp-adaptivity has demonstrated to perform much better than h-adaptivity. The main features of the goal oriented adaptivity with the S-parameters as the quantity of interest have been illustrated. Specifically, it is shown that the energy-norm is optimal when optimizing with respect to a reflection coefficient S_{ii}. When

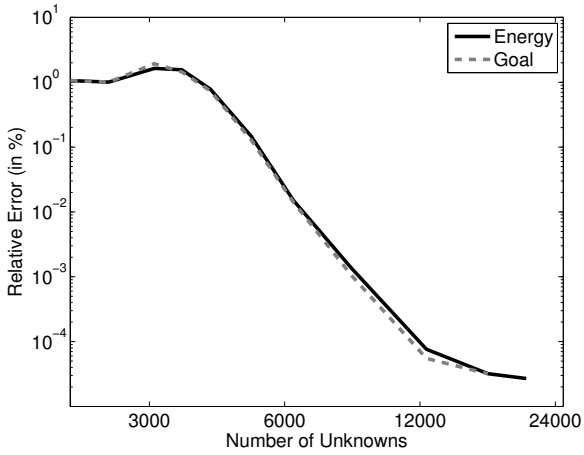

Figure 13. Convergence histories for the dielectric-slab filled waveguide with the energy-norm and with the goal-oriented adaptivity with S_{21} as the quantity of interest (lossless case)

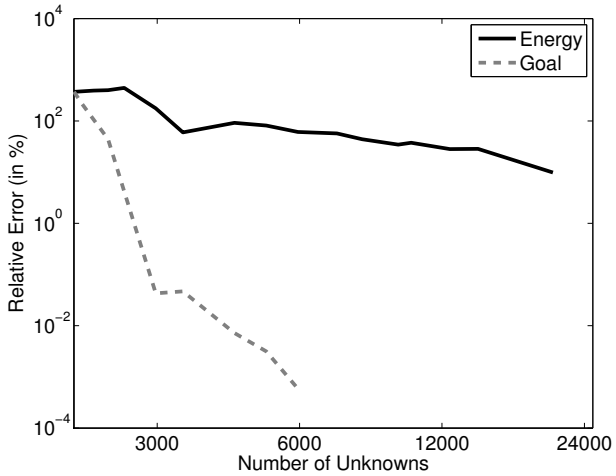

Figure 14. Convergence histories for the dielectric-slab filled waveguide with the energy-norm and with the goal-oriented adaptivity with S_{21} as the quantity of interest (lossy case; $\tan\delta = 1$)

the quantity of interest is a transmission parameter S_{ji} $(i \neq j)$ the goal-oriented is optimal. The goal-oriented adaptivity has been shown to clearly outperform the energy norm when the ports are not strongly coupled, as it happens in the presence of strong losses in the structure.

Acknowledgement

The authors wants to acknowledge the support of Ministerio de Educación y Ciencia of Spain under project TEC2007-65214/TCM.

Also, this material is based on research sponsored by the Air Force Research Laboratory, under agreement number FA8655-07-1-3041. The U.S. Government is authorized to reproduce and distribute reprints for Governmental purposes notwithstanding any copyright notation thereon. The views and conclusions contained herein are those of the authors and should not be interpreted as necessarily representing the

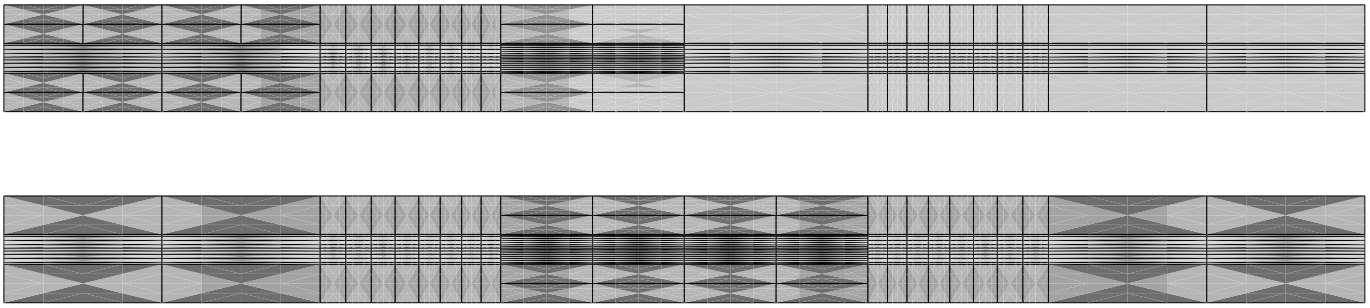

Figure 15. hp-grids obtained by using the energy norm —error of 0.5%— (top panel) and goal-oriented with S_{21} —error of 0.7%— (bottom panel) for the lossy dielectric-slab filled waveguide ($\tan\delta = 1$)

official policies or endorsements, either expressed or implied, of the Air Force Research Laboratory or the U.S. Government.

REFERENCES

[1] M. Salazar-Palma, T. K. Sarkar, L. E. García-Castillo, T. Roy, and A. R. Djordjevic, *Iterative and Self-Adaptive Finite-Elements in Electromagnetic Modeling*. Norwood, MA: Artech House Publishers, Inc., 1998.

[2] L. S. Andersen and J. L. Volakis, "Hierarchical tangential vector finite elements for tetrahedra," *IEEE Microwave and Guided Wave Letters*, vol. 8, no. 3, pp. 127–129, Mar. 1998.

[3] ——, "Adaptive multiresolution antenna modeling using hierarchical mixed-order tangential vector finite elements," *IEEE Transactions on Antennas and Propagation*, vol. 49, no. 2, pp. 211–222, Feb. 2001.

[4] J. P. Webb, "Hierarchal vector basis functions of arbitrary order for triangular and tetrahedral finite elements," *IEEE Transactions on Antennas and Propagation*, vol. 47, no. 8, pp. 1244–1253, Aug. 1999.

[5] D. K. Sun, J. F. Lee, and Z. Csendes, "Construction of nearly orthogonal nedelec bases for rapid convergence with multilevel preconditioned solvers," *SIAM Journal of Scientific Computing*, vol. 23, no. 4, pp. 1053–1076, 2003.

[6] J. P. Webb, "P-adaptive methods for electromagnetic wave problems using hierarchal tetrahedral edge elements," *Electromagnetics*, vol. 22, no. 5, pp. 443–451, Jul. 2002.

[7] S. C. Lee, J. F. Lee, and R. Lee, "Hierarchical vector finite elements for analyzing waveguiding structures," *IEEE Transactions on Microwave Theory and Techniques*, vol. 51, no. 8, pp. 1897–1905, Aug. 2003.

[8] Y. Zhu and A. C. Cangellaris, "Hierarchical finite element basis functions spaces for tetrahedra elements," in *Applied Computational Elecromagnetics Society (ACES) Meeting*, Monterey, CA, USA, Mar. 2001.

[9] A. Yu Zhu and C. Cangellaris, *Multigrid Finite Element Methods for Electromagnetic Field Modeling*, ser. IEEE Press Series on Electromagnetic Wave Theory. IEEE Press, 2006.

[10] M. M. Ilíc and B. M. Notaroš, "Higher order hierarchical curved hexaedral vector finite elements for electromagnetic modeling," *IEEE Transactions on Microwave Theory and Techniques*, vol. 51, no. 3, pp. 1026–1033, Mar. 2003.

[11] ——, "Higher order large-domain hierarchical FEM technique for electromagnetic modeling using Legendre basis functions on generalized hexaedra," *Electromagnetics*, vol. 26, no. 7, pp. 517–529, Oct. 2006.

[12] M. M. Ilíc, A. Ž. Ilíc, and B. M. Notaroš, "Efficient large-domain 2-D FEM solution of arbitrary waveguides using p-refinement on generalized quadrilaterals," *IEEE Transactions on Microwave Theory and Techniques*, vol. 53, no. 4, pp. 1377–1383, Apr. 2005.

[13] R. D. Graglia and G. Lombardi, "Singular higher order complete vector bases for finite methods," *IEEE Transactions on Antennas and Propagation*, vol. 52, no. 7, pp. 1672–1685, Jul. 2004.

[14] D.-K. Sun, L. Vardapetyan, and Z. Cendes, "Two-dimensional curl-conforming singular elements for FEM solutions of dielectric waveguiding structures," *IEEE Transactions on Microwave Theory and Techniques*, vol. 53, no. 3, pp. 984–992, Mar. 2005.

[15] J. P. Webb, "Singular tetrahedral finite elements for vector electromagnetics," *IEEE Transactions on Microwave Theory and Techniques*, vol. 55, no. 3, pp. 533–540, Mar. 2007.

[16] L. F. Demkowicz, P. Devloo, and J. T. Oden, "On an h-type mesh refinement strategy based on minimization of interpolation errors," *Computer Methods in Applied Mechanics and Engineering*, vol. 53, pp. 67–89, 1985.

[17] L. F. Demkowicz, J. T. Oden, W. Rachowicz, and O. Hardy, "Toward a universal $h-p$ adaptive finite element strategy, part 1: Constrained approximation and data structure," *Computer Methods in Applied Mechanics and Engineering*, vol. 77, pp. 79–112, 1989.

[18] L. F. Demkowicz, J. T. Oden, W. Rachowicz, and T. Westermann, "Toward a universal $h-p$ adaptive finite element strategy, part 2: A posterior error estimation," *Computer Methods in Applied Mechanics and Engineering*, vol. 77, pp. 113–180, 1989.

[19] W. Rachowicz, J. T. Oden, and L. F. Demkowicz, "Toward a universal $h-p$ adaptive finite element strategy, part 3: Design of $h-p$ meshes," *Computer Methods in Applied Mechanics and Engineering*, vol. 77, pp. 181–212, 1989.

[20] I. Babuška and M. Suri, "The p and $h-p$ versions of the finite elements approximation: Analysis of the optimal mesh sequences in one dimension," *Computer Methods in Applied Mechanics and Engineering*, vol. 80, pp. 5–26, 1990.

[21] P. R. B. Devloo, "A three-dimensional adaptive finite element strategy," *Computers & Structures*, vol. 38, no. 2, pp. 121–130, 1991.

[22] G. Zumbusch, "Simultaneous hp adaption in multilevel finite elements," Ph.D. dissertation, Freie Universität, Berlin, 1995, shaker Verlag, Aachen, 1996.

[23] P. R. B. Devloo, "PZ: An object oriented environment for scientific programming," *Computer Methods in Applied Mechanics and Engineering*, vol. 150, pp. 133–153, 1997.

[24] M. Ainsworth and B. Senior, "Aspects of an adaptive hp-finite element method: Adaptive strategy, conforming approximation, and efficient solvers," *Computer Methods in Applied Mechanics and Engineering*, vol. 150, pp. 65–87, 1997.

[25] F. Cugnon, "Automatisation des caculs Éléments finis dans le cadre de la méthode p," Ph.D. dissertation, Universite de Liege, 2000.

[26] L. Demkowicz, *Computing with hp Finite Elements. I. One- and Two-Dimensional Elliptic and Maxwell Problems*. Chapman & Hall/CRC Press, Taylor and Francis, Oct. 2006.

[27] M. Ainsworth and J. Coyle, "Hierarchic hp-edge element families for Maxwell's equations on hybrid quadrilateral/triangular meshes," *Computer Methods in Applied Mechanics and Engineering*, vol. 190, no. 49-50, pp. 6709–6733, 2001.

[28] P. D. Ledger, J. Peraire, K. Morgan, O. Hassan, and N. P. Weatherill, "Efficient highly accurate hp-adaptive finite element computations of the scattering width output of Maxwell's equations," *International Journal of Numerical Methods in Fluids*, vol. 43, pp. 953–978, 2003.

[29] C. Schwab, "Design of an hp-adaptive FE code for general elliptic problems in 3D," http://www.math.ethz.ch/research/groups/sam/projects/schwab/frauenfelder.

[30] L. E. García-Castillo, D. Pardo, and L. F. Demkowicz, "Fully automatic hp adaptivity for electromagnetics. application to the analysis of H-plane and E-plane rectangular waveguide discontinuities," in *2007 IEEE MTT-S International Microwave Symposium(IMS2007)*, Honolulu, Hawaii, Jun. 2007, session TU4F-04.

[31] J. Oden and S. Prudhomme, "Goal-oriented error estimation and adap-

tivity for the finite element method." *Computers and Mathematics with Applications*, vol. 41, no. 5-6, pp. 735–756, 2001.

[32] D. K. Sun, Z. Csendes, and J.-F. Lee, "Adaptive mesh refinement, h-version, for solving multiport microwave devices in three dimensions," *IEEE Transactions on Magnetics*, vol. 36, no. 4, pp. 1596–1599, Jul. 2000.

[33] P. Ingelström and A. Bondeson, "Goal-oriented error-estimation for S-parameter computations," *IEEE Transactions on Magnetics*, vol. 40, no. 2, pp. 1432–1435, 2004.

[34] I. Gómez-Revuelto, L. E. García-Castillo, D. Pardo, and L. F. Demkowicz, "A two-dimensional self-adaptive hp finite element method for the analysis of open region problems in electromagnetics," *IEEE Transactions on Magnetics*, vol. 43, no. 4, pp. 1337–1340, Apr. 2007.

[35] W. Rachowicz and L. Demkowicz, "An hp-adaptive finite element method for electromagnetics. Part 2: A 3D implementation," *International Journal for Numerical Methods in Engineering*, vol. 53, no. 1, pp. 147–180, 2002.

[36] L. Demkowicz, J. Kurtz, D. Pardo, M. Paszynski, W. Rachowicz, and A. Zdunek, *Computing with hp Finite Elements. II Frontiers: Three Dimensional Elliptic and Maxwell Problems with Applications*. Chapman & Hall/CRC Press, Taylor and Francis, 2007.

[37] L. F. Demkowicz, P. Monk, L. Vardapetyan, and W. Rachowicz, "De Rham diagram for hp finite element spaces," *Computer and Mathematics with Applications*, vol. 39, no. 7-8, pp. 29–38, 2000.

[38] D. Pardo, L. Demkowicz, C. Torres-Verdin, and L. Tabarovsky, "A goal oriented hp-adaptive finite element method with electromagnetic applications. Part I: Electrostatics," *International Journal for Numerical Methods in Engineering*, vol. 65, no. 8, pp. 1269–1309, Feb. 2006, see also ICES Report 04-57.

[39] I. Babuška and B. Guo, "Approximation properties of the hp-version of the finite element method," *Computer Methods in Applied Mechanics and Engineering*, vol. 133, pp. 319–346, 1996.

[40] J. M. Reiter and F. Arndt, "Rigorous analysis of arbitrarily shaped H- and E-plane discontinuities in rectangular waveguides by a full-wave boundary contour mode-matching method," *IEEE Transactions on Microwave Theory and Techniques*, vol. 43, no. 4, pp. 796–801, Apr. 1995.

[41] F. Arndt, J. Bornemann, and R. Vahldieck, "Design of multisection impedance-matched dielectric-slab filled waveguide phase shifters," *IEEE Transactions on Microwave Theory and Techniques*, vol. 32, no. 1, pp. 34–39, Jan. 1984.

Luis E. Garcia-Castillo was born in 1967 in Madrid, Spain. He received the degree of Ingeniero de Telecomunicación and the Ph. degree from the Universidad Politécnica de Madrid in 1992 and 1998, respectively. His Ph. thesis received two prizes from the Colegio Oficial de Ingenieros de Telecomunicación of Spain and the Universidad Politécnica de Madrid. From 1997 to 2000 he was an associate professor at the Universidad Politécnica de Madrid. From 2000 to 2005 he hold an associate professor position at the Universidad de Alcalá, Madrid, Spain. Since October 2005 he is with the Dep. of Signal Theory and Communications of the Universidad Carlos III de Madrid, Spain. His research activity and interests are focused in the application of numerical methods to high performance computational electromagnetics including finite elements, hp adaptivity, hybrid methods, and domain decomposition methods. He has authored 1 book, 5 contributions for chapters and articles in books, 18 articles in international journals, and 71 papers in international conferences, symposiums and workshops, plus a number of national publications and reports. He has leaded as principal Investigator three projects of the National Plan of Research of Spain and one of the regional Plan of Research of Madrid. He has also participated in 7 proyects and contracts, financed by international, european, and national institutions and companies.

David Pardo received the B.S. degree in mathematics from the University of The Basque Country, Spain, in 2000, and the M.S. and Ph.D. degrees in computational and applied mathematics from The University of Texas at Austin, in 2002 and 2004, respectively. Since then, he works as a Research Associate at the Petroleum and Geosystems Engineering at The University of Texas at Austin. His research interests include computational electromagnetics, petroleum-engineering applications (borehole simulations), adaptive finite-element methods, multigrid solvers, and inverse problems.

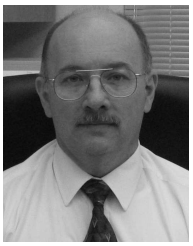

Leszek F. Demkowicz is a Professor in the Department of Aerospace Engineering and Engineering Mechanics at The University of Texas at Austin. Since 1993, he has served as an Assistant Director of the Institute for Computational Engineering and Sciences (ICES) at The University of Texas at Austin. He graduated cum laudae from Cracow University of Technology in 1976 with M.S. in Engineering Mechanics and from Jagiellonian University in Cracow in 1978 with M.S. in Theoretical Mathematics. He received a Ph.D.in Engineering in 1982 from The Cracow University of Technology, Poland. Dr. Demkowicz edited two books, has authored and co-authored two books, has published over 100 papers, and over 35 technical reports (unpublished elsewhere). He serves on the editorial board of four international journals. His area of expertise includes Functional Analysis, Numerical Analysis, h, p, and hp Adaptive Finite Element Methods with applications to solid and fluid mechanics, elasticity, acoustics and electromagnetic wave propagation.